Two-photon absorption in semiconductor nanocrystals

G. P. Banfi, V. Degiorgio, M. Ghigliazza, H. M. Tan,* and A. Tomaselli
Dipartimento di Elettronica, Università di Pavia, 27100 Pavia, Italy
(Received 23 May 1994)

Measurements of the two-photon absorption coefficient in semiconductor-doped glasses were performed. The imaginary part of the third-order optical susceptibility in the semiconductor particles is derived by combining nonlinear-optical-transmission data with small-angle neutron-scattering (SANS) results, which give the volume fraction of the nanocrystals. We find that the absorptive nonlinearity of the nanocrystals (with radii, also measured by SANS, in the range 2–11 nm) is close to that of the bulk semiconductor, in contrast to recent predictions and data.

In the last few years much attention was devoted to the effect of quantum confinement on near-resonant optical nonlinearities in semiconductors.[1,2] Semiconductor-doped glasses[1] (SDG's) were the most investigated materials, because of the possibility of obtaining crystallites of very small size with a relatively simple fabrication procedure, and also because of their potential interest for nonlinear-optical devices.[3,4] Differently from the resonant case, the optical nonlinearities at light frequencies well below the absorption edge are poorly understood. Cotter, Burt, and Manning[5] have recently presented calculations that predict a strong effect of the crystal size R on the third-order optical susceptibility $\chi^{(3)}$ for semiconductor nanocrystals below the band gap. In particular, the imaginary part of $\chi^{(3)}$, which is directly related to the two-photon absorption (TPA) coefficient β, is predicted to decrease when R decreases. However, the few available experimental results[5–7] would rather indicate the opposite behavior, with values of β for the crystallites typically five times larger than for the bulk semiconductor. Kang *et al.*[8] presented TPA spectra derived from luminescence data, and pointed out the necessity of including valence-band mixing in the calculation of the energy levels of nanocrystals. In order to clearly establish the effect of confinement on the magnitude of TPA below the band gap, it is necessary to obtain accurate optical data on a wide range of nanocrystal sizes and on the whole interval of accessible ratios $y=E_g/(\hbar\omega)$, where E_g is the energy gap of the SDG and $\hbar\omega$ is the energy of the incident photon. It is also essential to complement the optical measurements with a careful structural characterization of the SDG's used.

In this paper we report measurements of $\mathrm{Im}\chi^{(3)}$ in a series of SDG's.[9] Our data cover a range of R between 2 and 11 nm, and a range of y between 1 and 1.9. We find that, in order to extract the imaginary part of $\chi^{(3)}$ from the optical transmission data in the picosecond time regime, it is necessary to take into account free-carrier-absorption (FCA) processes. We have also performed experiments in the femtosecond time domain where the effect of FCA is negligible. The average size and the volume fraction of nanocrystals were measured by small-angle neutron scattering (SANS). The values of $\mathrm{Im}\chi^{(3)}$ obtained for the nanocrystals are comparable to those of the bulk semiconductors of similar composition, indicating that quantum confinement effects on TPA, at least in the investigated size range, are very small.

The list of used SDG's, all manufactured by Schott Glaswerke (Mainz, Germany) and commercialized as sharp cutoff optical filters, is given in Table I. The number which identifies the glass corresponds to the cutoff wavelength λ_c in nanometers, with an uncertainty of ± 6 nm. The samples with $495 \leq \lambda_c \leq 715$ nm contain $CdS_{1-x}Se_x$ crystallites with different stoichiometry, and the infrared filters, samples RG830 and RG850, contain CdTe crystallites.

The SANS data were taken at the Cold Neutron Facility of the National Institute of Standards and Technology, Gaithersburg, Maryland. Details on the SANS experiment are reported elsewhere.[10] Neutron scattering represents a very useful technique for the structural characterization of SDG's because of the strong mismatch in the neutron-scattering amplitude between the nanocrystals and the glass matrix.[11] The average crystallite radius R is derived from the angular dependence of the scattered

TABLE I. TPA coefficient of SDG's (third column); volume fraction of the nanocrystals (fourth column); TPA coefficient of the nanocrystals (fifth column). In the second column, P denotes measurements at 1.06 μm with 30-ps pulses, F denotes measurements at 0.6 μm with 180-fs pulses. When a range of β values is given, the first value is derived by taking $\sigma=2\times10^{-18}$ cm^2, and the second by taking $\sigma=0$.

Sample		$\beta_{SDG}\times10^3$ (cm/GW)	f_v ($\times10^3$)	β_m (cm/GW)
OG570	P	2–8	3.5	1.1–4.3
OG590	P	3–10	4.7	1.3–4.3
RG610	P	4–12	2.9	2.8–8.3
RG630	P	9–27	3.2	6.2–18
RG665	P	15–40	3.5	9.5–25.5
RG695	P	9–25	1.6	12.5–34.8
RG715	P	18±3	3.2	12.7±2.1
RG830	P	17±3	1.6	32.5±5.9
RG850	P	23±2	1.5	47±4
GG495	F	15±3	5.2	6.3±1.3
OG570	F	23±3	3.5	12.5±1.6
OG590	F	20±5	4.7	10.1±2.5

intensity, and the volume fraction occupied by the crystallites, f_v, is obtained from the absolute value of the scattered intensity, which is proportional to $f_v R^3$.[10,11] It should be noted that f_v cannot be derived from a chemical analysis of the SDG's because a significant fraction of the semiconductor constituents is still dispersed in the glass matrix.

Nonlinear-transmission measurements were performed on all samples by employing 30-ps pulses (repetition rate 1 Hz) at 1.06 μm from a Nd-YAG (yttrium aluminum garnet) mode-locked laser. The pulse duration was measured by standard correlation techniques. The beam quality factor, obtained by monitoring the transversal intensity profile of the laser beam with a charge-coupled device camera, was $M^2=1.25$. Typically, the thickness of the samples was 3–5 mm, but for a few SDG's we also used much thicker samples.

The transmission T, measured as the ratio between the transmitted energy and the input energy, is shown in Fig. 1 as a function of the peak intensity Φ_0. The decrease of T with Φ_0 is due to TPA processes, which become possible when $y \leq 2$. We find indeed that the nonlinear absorption of the Nd-YAG laser pulses becomes undetectable for SDG's with $\lambda_c \leq 550$ nm. It should be noted that the glass matrix, with its large band gap, plays no role in TPA. In the presence of TPA, the intensity Φ of a pulse propagating along z is given, neglecting diffraction, by

$$\frac{d\Phi(r,z,t)}{dz} = -\beta\Phi^2(r,z,t) - \sigma N(r,z,t)\Phi(r,z,t) , \quad (1)$$

where r is the radial coordinate and β is the TPA coefficient, which is related to $\mathrm{Im}\chi^{(3)}$ by the expression $\beta=\omega(\varepsilon_0 c^2 n^2)^{-1}\mathrm{Im}\chi^{(3)}$, n being the index of refraction. The second term at the left-hand side of Eq. (1) accounts for FCA, with N the free carrier density generated by TPA and σ denoting the related cross section. Assuming the decay of N to be negligible during the pulse duration (the validity of this assumption is supported by time-resolved degenerate-four-wave-mixing measurements we performed on the same samples), N can be calculated through

$$N(r,z,t) = \int_{-\infty}^{t} \frac{\beta\Phi^2(r,z,t')}{2\hbar\omega} dt' . \quad (2)$$

By assigning the spatial-intensity profile and the temporal shape of the pulse, the nonlinear dependence of the output energy as a function of the input energy can be calculated by solving numerically Eqs. (1) and (2). In principle, the two parameters β and σ could be obtained by a best fit to the data taken with a single sample of thickness L. However, because of the limited range of input energies over which the nonlinear transmission can be investigated and because of the uncertainties associated with the experimental data, it is not possible to extract reliably the two parameters from a single experimental curve. For instance, the data points referring to the OG570 sample in Fig. 1 can be described, with no appreciable difference in the quality of the fit, by adopting any couple of values within the interval $\beta=8\times10^{-3}$ cm/GW, $\sigma=0$; $\beta=2\times10^{-3}$ cm/GW, $\sigma=2\times10^{-18}$ cm^2. It should be noted that, for $\sigma=0$, the transmission derived from

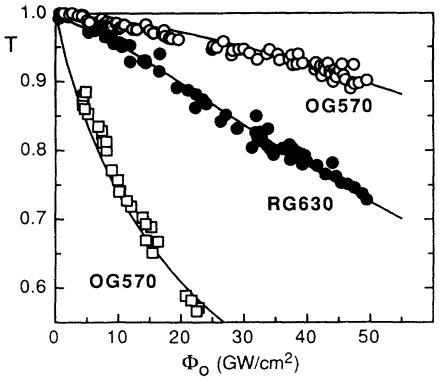

FIG. 1. Transmission vs peak intensity for some SDG's. The two upper sets of data points (○ and ●) are taken with 30-ps pulses at 1.06 μm with a sample thickness of 0.8 cm. The lower set of data points (□) is taken with 180-fs pulses at 0.6 μm with a sample thickness of 5 cm. Full lines are best-fit curves.

Eq. (1) depends on the peak intensity Φ_0 and on L only through the product $\Phi_0 L$. In Fig. 2 we show plots of T vs $\Phi_0 L$ for two different sample thicknesses. The two sets of data do not fall on the same curve, which indicates that FCA cannot be neglected. A fit to both sets of data allows one to derive β and σ. Adopting this procedure, we estimated $\sigma\approx2\times10^{-18}$ cm^2 for both samples RG830 and RG715. The value is consistent with $\sigma=1.95\times10^{-18}$ cm^2 derived for sample RG850 in Ref. 6.

A simple way to reduce the effect of FCA is that of measuring the nonlinear transmission with ultrashort pulses, which can provide a high enough intensity to evidence TPA without exciting too many carriers during the pulse duration. Numerical solutions of Eqs. (1) and (2) indicate that, for an extended range of values of L, Φ_0, and σ, the effect of FCA can safely be disregarded with pulses shorter than 200 fs. The ultrashort pulse measurements were performed at the European Laboratory for Nonlinear Spectroscopy, Florence, Italy. Our investigation was limited to samples GG495, OG570, and OG590, because only the wavelength of 605 nm ($\hbar\omega=2.06$ eV) was available at the time of the experiment. The 190-fs pulse (spectral width 4.2 nm, repetition rate 10 Hz) from the dye laser amplifier, after passing through a spatial

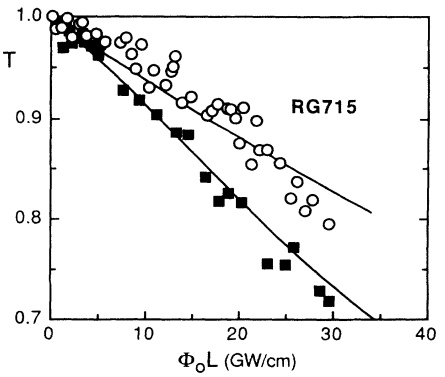

FIG. 2. Transmission vs $\Phi_0 L$ for two distinct values of L: ■, $L=0.8$ cm; ○, $L=5$ cm. Full lines are best-fit curves.

filter, was gently focused to provide ≈ 10 μJ of energy within a smooth Airy disc at the sample. A good accuracy in the measurement of T was achieved by using a differential detector and a reference beam. A cross-check of the absolute calibration (which required measuring energy, beam shape, and pulse duration) was given by a separate experiment in which we observed the beam depletion due to second-harmonic generation in a 0.5-mm-thick potassium dihydrogen phosphate (KDP) platelet, in type-I phase matching [using KDP as a TPA standard, we assumed d_{36} (KDP) = 0.4 pm/V]. Since beam depletion due to second-harmonic generation is formally equivalent to that due to TPA, such a calibration procedure is simple and reliable. We found some evidence of a darkening effect[1] (especially with sample GG495): that is, starting with a fresh sample, the linear transmission showed an initial decrease with time before stabilizing after exposure. We relied on predarkening to avoid changes of the linear transmission during data collection. A typical transmission curve can be seen in Fig. 1.

The values of β_{SDG} derived from the transmission data are reported in Table I. For those measurements performed with 30-ps pulses in which it was not possible to derive both β and σ, we fixed σ by considering the two extreme scenarios of $\sigma=2\times10^{-18}$ cm^2 and $\sigma=0$. There is some indication[6] that σ decreases as E_g increases, so that the value $\sigma=0$ is probably more appropriate for the largest values of y.

The few published values of β_{SDG} are rather different among themselves and are all larger than our data. The origin of the discrepancy with Ref. 5 is probably that FCA was not taken into account in the interpretation of transmission data. In the case of Ref. 7, the used technique does not allow an easy absolute calibration. The origin of the discrepancy with Ref. 6 is unclear.

The relation between the measured $\chi^{(3)}_{SDG}$ of the composite SDG, and $\chi^{(3)}_m$ of the nanocrystals, is given by[1,2]

$$\chi^{(3)}_{SDG}=\chi^{(3)}_m f^4 f_v \ , \tag{3}$$

where f is the local-field correction factor. Assuming a spherical shape and an isotropic polarizability for the crystallites, f is given by $f=3n_g^2/(n_m^2+2n_g^2)$, where n_g is the index of refraction of the glass matrix and n_m that of the crystallite. At 1.06 μm, f was calculated by taking $n_g=1.53$; $n_m=2.84$ (value of bulk CdTe) for samples RG830 and RG850; $n_m=2.33$ (value of bulk CdS) for sample GG495, $n_m=2.54$ (value of bulk CdSe) for sample RG715, and then interpolating according to λ_c for the others glasses of the $CdS_{1-x}Se_x$ series. At 0.6 μm, n_m is about 3% larger and f^4 somewhat lower.

By using Eq. (3) we can write $\beta_{SDG}=\beta_m(n_m^2/n_{SDG}^2)f^4 f_v$. This relation allows one to derive β_m from the measured β_{SDG} and f_v. The obtained values are given in Table I. Taking into account all the uncertainties, we estimate that the absolute calibration of β_m in our experiment is correct within a factor of 2.

The comparison between the TPA coefficient of nanocrystals and that of bulk semiconductors is shown in Fig. 3, where we plotted the scaled quantity $(\omega/\omega_0)^4 \mathrm{Im}\chi^{(3)}$, with ω_0 the frequency of 1.06-μm radiation, as a function

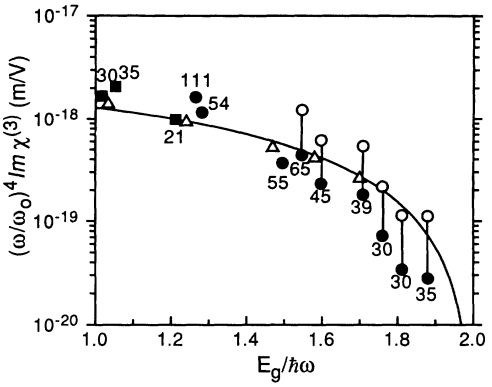

FIG. 3. Plot of the scaled quantity $(\omega/\omega_0)^4$ Im$\chi^{(3)}$ vs $E_g/(\hbar\omega)$. ■, optical measurements at 0.6 μm. Circles refer to optical measurements at 1.06 μm assuming $\sigma=2\times10^{-18}$ cm^2 ●, $\sigma=0$ (○). The numbers associated to the experimental points are the radii of the nanocrystals in Å △, experimental data for bulk semiconductors, taken from Refs. 14 and 15, all measured at 1.06 μm, except for the point corresponding to the lowest value of $E_g/(\hbar\omega)$, which is measured at 0.53 μm. The solid line is the behavior of $(\omega/\omega_0)^4$Im$\chi^{(3)}$ predicted for bulk semiconductors.

of $E_g/(\hbar\omega)$. For the nanocrystals, we set $E_g=hc/\lambda_c$. Such a value of E_g should differ by no more than 20 meV from the value one would derive from the wavelength of the fluorescence peak at room temperature,[12] and practically coincides with the energy difference between the higher discrete level of the valence band and the lower one of the conduction band. Due to the blueshift caused by confinement, the nanocrystals and the bulk with the same E_g do not have exactly the same stoichiometry. The distinction is irrelevant for present purposes, except at the highest $E_g/(\hbar\omega)$ values. The full curve in Fig. 3 gives the bulk values, calculated by using the relation

$$\mathrm{Im}\chi^{(3)}=\mathrm{const}\times(1/\omega E_g^3)(1-2\hbar\omega/E_g)^{3/2}(2\hbar\omega/E_g)^5 \ ,$$

which was proposed by Sheik-Bahae, Hagan, and Van Stryland.[13] The constant in the expression of Im$\chi^{(3)}$ is fixed by fitting the curve to experimental data for bulk semiconductors,[14,15] which are also reported in Fig. 3.

We find that Im$\chi^{(3)}_m$ decreases monotonically as y increases. Within experimental error, TPA in the nanocrystals has the same behavior as in the bulk semiconductor. Quantum confinement effects on Im$\chi^{(3)}_m$ must be quite small, if we note that deviations from the bulk values are not evident even for the small crystallites of the sample GG495 ($R=2$ nm). Using the R and y parameters of this sample, the theoretical curves plotted in Fig. 1 of Ref. 5 predict Im$\chi^{(3)}_m$ to be at least four times smaller than for the bulk.

The reason for Im$\chi^{(3)}_m$ to decrease in the nanocrystal is attributed by Cotter, Burt, and Manning[5] to the fact that, in the sum-over-states formula leading to $\chi^{(3)}_m$, the expectation value for the interaction term $-e/m$ **A**·**p** vanishes in bound states of the nanocrystal contrary to the case of bulk. It is not clear, however, why such a fact should be so relevant when $2\hbar\omega$ is above E_g by several discrete levels. Different, of course, is the situation when $2\hbar\omega$ is

closer to E_g, since a decrease of R increases the gap and TPA can vanish at the limit.

We also performed some preliminary measurements of $|\chi^{(3)}_{SDG}|$ through nearly degenerate three-wave mixing at wavelengths around 1 μm. We found that the ratio $|\chi^{(3)}_{SDG}|^2/|\chi^{(3)}_{glass}|^2$ takes values in the interval 1–2 depending on the SDG. This result, quite at variance with data in Ref. 5, indicates a significant contribution of the glass matrix and, making use of Eq. (3), appears to be fairly consistent with the published value of $\chi^{(3)}_b$ of the bulk semiconductor.

In conclusion, we have shown that for semiconductor nanocrystals with a size ranging between 2 and 11 nm, the TPA coefficient is close to that of the bulk semiconductor in the whole accessible range of $E_g/(\hbar\omega)$ values. Such a result calls for further efforts toward a quantitative theoretical treatment of below-band-gap optical nonlinearities in confined systems.

We thank the European Laboratory for Nonlinear Spectroscopy, and, in particular, R. Righini and E. Sa'nta, for making available the femtosecond laser equipment. We acknowledge financial support from the Italian Ministry for University and Research (MURST 40% funds) and from Progetto Finalizzato Telecomunicazioni of the Consiglio Nazionale delle Ricerche (Italy).

*Permanent adress: Changchun Institute of Optics and Fine Mechanics, Academia Sinica, Changchun, Jilin, China.

[1]C. Flytzanis, F. Hache, M. C. Klein, D. Ricard, and P. Roussignol, Prog. Opt. **29**, 323 (1991).

[2]S. Schmitt-Rink, D. A. B. Miller, and D. S. Chemla, Phys. Rev. B **35**, 8113 (1987).

[3]N. Finlayson, W. C. Banyai, C. T. Seaton, G. L. Stegeman, M. O'Neill, T. G. Cullen, and C. N. Ironside, J. Opt. Soc. Am. B **6**, 675 (1989).

[4]J. Yumoto, S. Fukushima, and K. Kubodera, Opt. Lett. **12**, 832 (1987).

[5]D. Cotter, M. G. Burt, and R. J. Manning, Phys. Rev. Lett. **68**, 1200 (1992).

[6]S. M. Oak, K. S. Bindra, R. Chari, and K. C. Rustagi, J. Opt. Soc. Am. B **10**, 613 (1993).

[7]R. Tommasi, M. Lepore, and I. M. Catalano, Solid State Commun. **85**, 539 (1993).

[8]K. I. Kang, B. P. McGinnis, Sandalphon, Y. Z. Hu, S. W. Koch, N. Peyghambarian, A. Mysyrowicz, L. C. Liu, and S. H. Risbud, Phys. Rev. B **45**, 3465 (1992).

[9]Some preliminary results were presented by G. P. Banfi, M. Ghigliazza, H. M. Tan, and S. Tomaselli, in *Quantum Electronics and Laser Science,* Vol. 13 of *1992 OSA Technical Digest Series* (Optical Society of America, Washington, D.C., 1992), p. 448, paper PTh 48.

[10]G. P. Banfi, V. Degiorgio, A. R. Rennie, and J. G. Barker, Phys. Rev. Lett. **69**, 3401 (1992); G. P. Banfi, V. Degiorgio, and B. Speit, J. Appl. Phys. **74**, 6925 (1993).

[11]V. Degiorgio, G. P. Banfi, G. Righini, and A. R. Rennie, Appl. Phys. Lett. **57**, 2879 (1990).

[12]N. F. Borrelli, D. W. Hall, H. J. Holland, and D. W. Smith, J. Appl. Phys. **61**, 5399 (1987).

[13]M. Sheik-Bahae, D. J. Hagan, and E. W. van Stryland, Phys. Rev. Lett. **65**, 96 (1990).

[14]E. W. Van Stryland, M. A. Woodhall, H. Vanherzele, and M. J. Soileau, Opt. Lett. **10**, 490 (1985).

[15]A. A. Said, M. Sheik-Bahae, D. J. Hagan, T. H. Wei, J. Young, and E. W. van Stryland, J. Opt. Soc. Am. B **9**, 405 (1992).